Permeation of Dissolved Carbon Dioxide in Synthetic Membranes

TSUTOMU NAKAGAWA,* ATSUKO NARUSE, and AKON HIGUCHI

Department of Industrial Chemistry, Meiji University, 1-1-1 Higashi-mita, Tama-ku, Kawasaki, Kanagawa 214, Japan

SYNOPSIS

Permeability coefficients of dissolved carbon dioxide in poly(dimethyl siloxane), plasma-treated poly(dimethyl siloxane) membranes, and other membranes were measured by applying a carbon dioxide electrode in a liquid to liquid diffusion cell. The apparent permeability coefficients of carbon dioxide polystyrene, low density polyethylene, and nylon membranes in a liquid phase were observed to be higher than those in a gas phase due to a plasticizing effect of water molecules in the membranes. Boundary layer's resistance was estimated for plasma-treated and nontreated poly(dimethyl siloxane) membranes. The plasma treatment (10 W for 1 min in this study) which makes hydrophilic surfaces without change of bulk polymer properties was found to be effective to decrease the boundary layer's thickness and to increase the apparent permeability coefficient in the liquid phase.

INTRODUCTION

Permeabilities of dissolved oxygen in membranes have been studied as a basis for contact lens applications.[1-7] The permeability of dissolved oxygen is mostly determined by applying an oxygen electrode in a liquid to liquid diffusion cell. The permeability coefficient is known to increase with increasing a membrane thickness due to the boundary layer's effect,[1,4,6] whereas the permeability coefficient in a dry membrane does not depend on the membrane thickness.

One of the authors[8,9] developed an apparatus for the measurement of gas permeabilities in hydrogels using a vacuum line technique. The permeabilities of gases in hydrogels have been reported in several membrane systems by several researchers.[8-11] The permeability coefficients were reported to be independent of membrane thickness in this method,[8] since there is no boundary water resistance in these systems.

Few researchers[12] studied transport of dissolved gas except oxygen in the membranes using a gas electrode. Izydorczyk et al.[12] reported diffusion coefficients of dissolved carbon dioxide through several membranes by the time lag method, but they did not measure any of permeability. This work deals with the permeability coefficients of dissolved carbon dioxide in poly(dimethyl siloxane), plasma-treated poly(dimethyl siloxane) membranes, and other membranes measured by applying a carbon dioxide electrode in a liquid to liquid diffusion cell. We discuss the effect of the boundary layer's resistance that exists in the membrane–water interface for both poly(dimethyl siloxane) and plasma-treated poly(dimethyl siloxane) membranes.

EXPERIMENTAL

Materials

Poly(dimethyl siloxane) membranes (Silastic, 500-1, 3, 5 and 7, Dow Corning Ltd.) (PDMS), polystyrene membranes (Stylex, Mitsubishi Plastics Ind. Ltd.) (PSt), low density polyethylene (LDPE), and nylon 6 membranes were used in this study. CO_2 of more than 99.99% purity was used as received. Ultrapure water by Toraypure LV-10T reverse osmosis system (Toray Co., Ltd.) was used throughout the experiments.

* To whom correspondence should be addressed.

Journal of Applied Polymer Science, Vol. 42, 383-389 (1991)
 CCC 0021-8995/91/020383-07$04.00

Plasma Treatment

Some PDMS membranes were treated with plasma discharge. The reactor for the plasma treatment was similar to that reported by other investigators.[13] The reactor had a 25 cm diameter and was 30 cm high with operating frequency of 13.56 MHz. The membranes were exposed to an oxygen plasma for 1 min at 10 or 50 W.

Apparatus and Procedure

Permeation Apparatus

A diagram of the permeation apparatus is shown in Figure 1. The permeation cell consists of two glass chambers separated by a membrane. The cell volume of the upstream or downstream side is 200 ml, respectively. The effective membrane area is 6.84 cm^2. The revolution speed of magnetic spinbars in the cells was controlled (i.e., 430 rpm in this study) by a magnetic stirrer having a revolution meter (HS-3D, Iuchi Seiseido Co., Ltd.).

After water in the cells was equilibrated with CO_2 atmospherically, the upstream water was pumped out and saturated water with CO_2 at 1 atm was immediately injected into the upstream side cell at time = 0 s. Permeability coefficients were calculated from the concentration change of CO_2 monitored by the CO_2 electrode.

Description of the Sensor and Principle of Operation

The pH-type CO_2 electrode made by TOA Electronics Ltd. was used as a sensor to determine the concentration of carbon dioxide. A diagram of the electrode is shown in Figure 2. The carbon dioxide electrode is a so-called combination electrode which consists (1) of a glass electrode as a measuring electrode with a high sensitive glass membrane for pH change and (2) a silver–silver chloride electrode as a reference electrode. The bottom of the glass electrode detects the slight pH change within a thin spacer (3). The sheath is made of a poly(methyl methacrylate) and filled with an $NaHCO_3$ and NaCl solution (5) enough to ignore the concentration increase of HCO_3^-, which is newly formed with the CO_2 permeating.

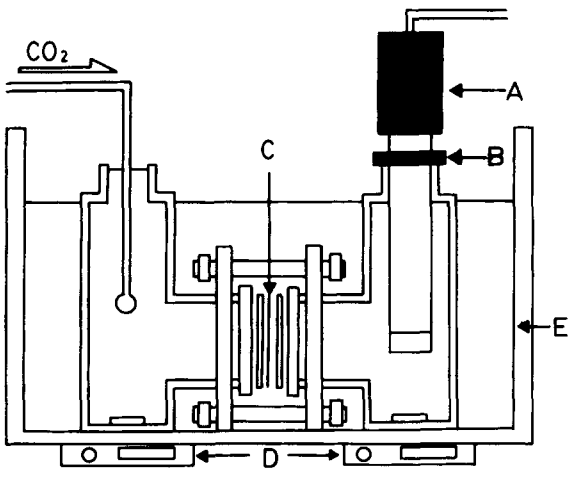

Figure 1 Diagram of permeation apparatus: (A) CO_2 electrode; (B) O-ring; (C) membrane; (D) magnetic stirrer; (E) water bath.

The concentration of permeated CO_2 is determined as follows: The carbon dioxide which was permeated to the downstream side dissolved and reached equilibrium in the internal filling solution:

$$CO_2 + H_2O \rightleftarrows H_2CO_3 \rightleftarrows H^+ + HCO_3^- \quad (1)$$

and the dissociation constant at 25°C is

$$K = \frac{[H^+][HCO_3^-]}{[CO_2]} = 4.3 \times 10^{-7} \quad (2)$$

Then,

$$\log K = \log[H^+] + \log[HCO_3^-] - \log[CO_2] \quad (3)$$

$$pK = -\log K \quad \text{and} \quad pH = -\log[H^+]$$

Therefore,

$$pH = pK + \log[HCO_3^-] - \log[CO_2] \quad (4)$$

The carbon dioxide which permeated through the membrane decreased pH. The concentration of HCO_3^- was kept constant as mentioned before, which made $pK + \log[HCO_3^-]$ constant. In the internal filling solution, therefore,

$$pH = \text{const} - \ln[CO_2] \quad (5)$$

The pH changes were monitored by differences of the electromotive forces with the reference electrode. This is expressed as follows:

$$E = E_0 + k \ln a_{H^+} \quad (6)$$

where E is the electromotive force obtained experimentally, E_0 is an intrinsic electromotive force in this system, k is $RT \ln 10/(ZF)$ ($Z = 1$ in this case), and a_{H^+} is an activity of H^+. F is the Faraday constant. Equation (6) is also expressed as follows:

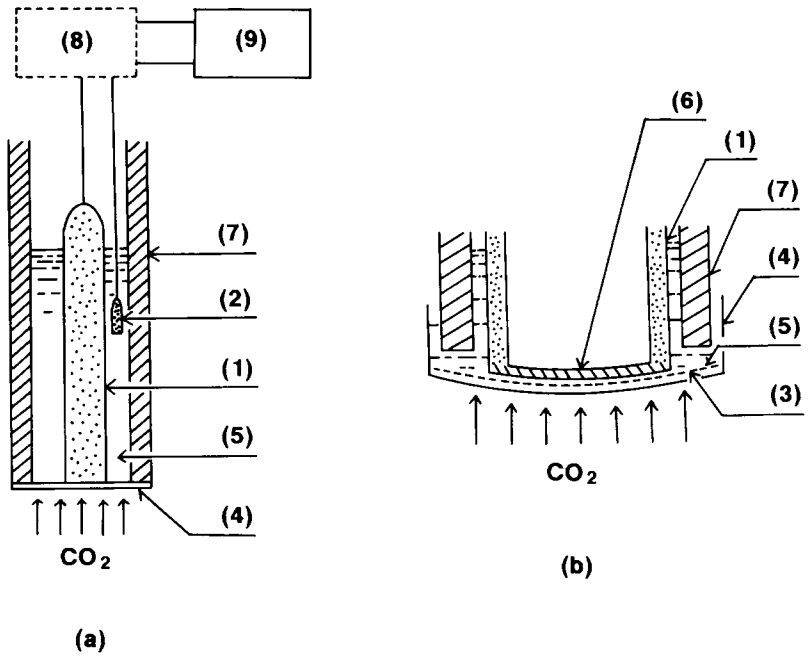

Figure 2 Schematic diagram of carbon dioxide electrode. (a) Section: (1) glass electrode; (2) reference electrode; (4) permeable membrane; (5) internal filling solution; (6) high sensitive glass membrane; (7) sheath; (8) impedance converter; (9) detector. (b) Bottom: (1) glass electrode; (3) spacer; (4) permeable membrane; (5) internal filling solution; (6) high sensitive glass membrane; (7) sheath.

$$E = E_0 + k \ln(rC_1) \quad (7)$$

$$= E_0 + k \ln r + k \ln C_1 \quad (8)$$

where r is an activity coefficient.

$$C_1 = 10^{(E-E_0')/k} \quad (9)$$

where $E_0' = E_0 + k \ln r$. Figure 3 shows the relationship between the concentration of CO_2 in the outer solution of the electrode and E. The experiments were performed on the condition of pH $\doteqdot$ 7.0 at the downstream side; the self-dissociation of water was neglected. Under this pH range, the existence of CO_3^{2-} was also negligible. k is obtained from the slope of proportional parts in Figure 3, experimentally. The problems of the divalent ions such as CO_3^{2-} and $2H^+$ on the experimental results were also solved by using the calibration curve.

An apparent permeability coefficient for each membrane thickness, P, is finally expressed by

$$P = L(dC/dt)V/[A(p_0 - C_1/\alpha)] \quad (10)$$

where L is the membrane thickness, A is the membrane area, V is the cell volume at the downstream side, p_0 is the CO_2 partial pressure at the upstream side (76 cm Hg in our study), and α is the Bunsen constant (0.759 cm Hg^{-1} at 25°C).[14] The permeability coefficient was determined from the mean values of three to five experiments. All measurements were performed at 25 ± 0.1°C.

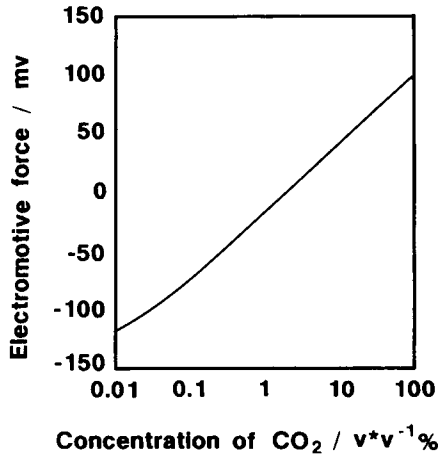

Figure 3 Plot of electromotive force vs. concentration in gas phase for carbon dioxide electrode at 25°C in this system.

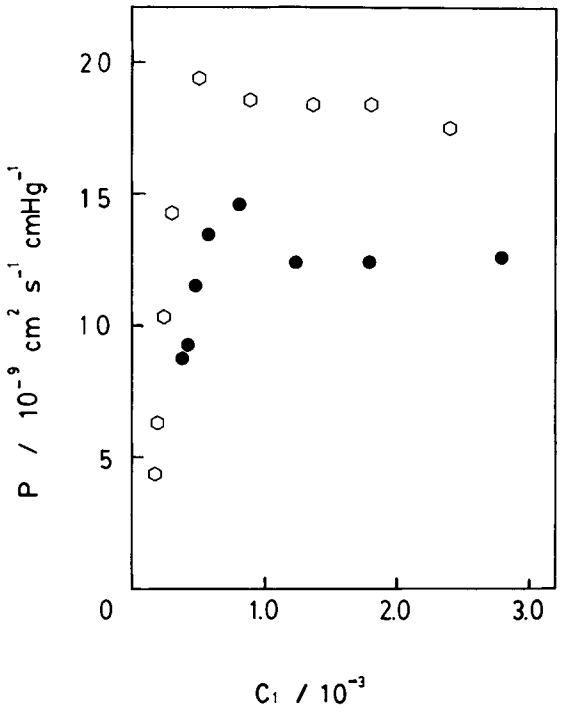

Figure 4 Dependence of permeability coefficients of CO_2 on C_1 for LDPE (○) and PSt (●) membranes at 25°C and p_0 = 1 atm.

RESULTS AND DISCUSSION

Figure 4 shows the dependence of apparent permeability coefficients on C_1 for LDPE and PSt membranes. Both membranes show the permeability coefficient increases with the increasing C_1 at C_1 < 0.001 (cm^3(STP)/cm^3) and give a maximum near C_1 = 0.001. This phenomenon probably arises from the slow response time of the electrode at the low concentration of CO_2. It was reported that it took 12 min from atmospherical concentration of CO_2 (0.0003 cm^3(STP)/cm^3) to C_1 = 0.001 and 4 min from the atmospherical concentration to C_1 = 0.01 to show the actual potential by the electrode.[15] The apparent permeability coefficient shows lower values due to the limit of response time at the beginning (C_1 < 0.001). When C_1 increases at the concentration below the maximum, the response rate becomes faster to catch up with the increasing rate of CO_2 at the downstream side, and this contributes to the increase of the apparent permeability coefficient. When C_1 comes near the maximum, the response rate gives a rather faster rate compared with the increasing rate of CO_2 concentration at the downstream side. This contributes to the higher apparent permeability coefficient than the actual permeability coefficient where P calculated by eq. (10) indicates the response rate rather than the permeating rate of CO_2. Each curve in Figure 4 is, therefore, found to have the maximum permeability coefficient. The permeability coefficient is finally observed to be independent of C_1 at C_1 > 0.001, because the measured potential coincides with the actual potential without any time lag due to the fast response time of the electrode.

Dependence of apparent permeability coefficient on C_1 for PDMS membranes is shown in Figure 5. A similar tendency that the permeability coefficients at C_1 < 0.001 show smaller permeability coefficients than those at C_1 > 0.001 is observed. The independent permeability coefficients of C_1 observed at C_1

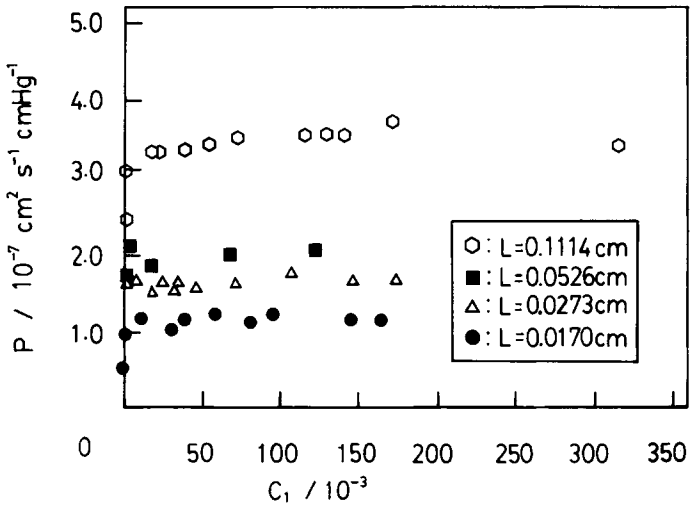

Figure 5 Dependence of permeability coefficients of CO_2 on C_1 for PDMS membranes at 25°C and p_0 = 1 atm.

> 0.001 are considered to be the true permeability coefficients of dissolved CO_2 for each membrane and are summarized in Table I. The permeability coefficients of CO_2 through the membranes that are measured in a gas phase (high vacuum method) are also shown in Table I as a comparison of permeability coefficients measured in the liquid phase and in the gas phase.

It is known that there exists a boundary layer resistance on the membrane interface in the liquid phase,[1,4,6] and this resistance may contribute to the lower permeability than the value measured in the gas phase. Table I shows, however, that the apparent permeability coefficients in the liquid phase are higher than those in the gas phase for the membranes having the same thickness except PDMS at $L < 0.1$ cm. This phenomenon is observed not only on the hydrophilic membrane, nylon, but on hydrophobic membranes such as PSt and LDPE. Since the lowest permeability coefficient capable of being measured in the liquid phase is estimated to be 1×10^{-11} $cm^3(STP)cm/cm^2$ s cm Hg from the blank test, the higher permeability coefficients observed in the liquid phase is not due to the leak of CO_2 at the downstream side. The permeability coefficient of the nylon membrane in the liquid phase is especially observed to be 2 orders faster than the permeability coefficient in the gas phase. This phenomenon can be explained by the plasticizing effect[16,17] due to water molecules in the membrane. The plasticizing effect is predominant over the reduction of the permeability due to the boundary layer's resistance, and this results in the higher permeability in the liquid phase. PDMS membranes having $L < 0.1$ cm are, on the contrary, observed to have higher permeability in the gas phase than that in the liquid phase. Since the PDMS membranes are more than 2 orders faster than LDPE, PSt, and nylon membranes from Table I, the boundary layer resistance should be more effective than the plasticizing effect for the membranes having high permeability and hydrophobic characteristics at thin membrane thickness.

Permeability coefficients in PDMS membranes in the liquid phase are observed to increase with the increasing membrane thickness from Table I. It is known that there exists a boundary layer resistance at the interface between the membrane and water.[1,4,6] As the membrane thickness becomes thinner, the contribution of boundary layer resistance becomes more significant, and this leads to the lower permeability. The boundary layer resistance is known not to be eliminated by a fast stirring rate.[1] The boundary layer resistance and the true permeability coefficient in the water phase that excludes the effect of boundary layer resistance can be obtained from eq. (11) derived by Hwang et al.[6]:

$$1/P = 1/\mathrm{DS} + R_w/L \qquad (11)$$

where DS is the true permeability coefficient of membrane, R_w is the boundary layer resistance, and P is the permeability coefficient obtained experimentally from eq. (10). R_w and DS can be obtained from the slope and the intercept in the plots of P^{-1} vs. $1/L$.

Figure 6 shows plots of P^{-1} vs. $1/L$ for nontreated PDMS membranes. DS and R_w are calculated using a least squares method and summarized in Table II.

Flux is known to be inversely related to the membrane thickness in the gas phase. Flux in the liquid phase, on the contrary, is limited to the finite value of boundary layer resistance with $L \rightarrow 0$. Elimination of boundary layer's resistance leads to membranes having high flux in the liquid phase. One may wonder whether the boundary layer resistance is characteristic of membrane materials and whether it depends on the hydrophilicity (or hydrophobicity) of the membrane surfaces. It is known that plasma treatment induces several hydrophilic groups on the

Table I Permeability Coefficients of CO_2 in Various Membranes at 25°C[a]

Membrane	L/cm	P in Gas Phase	P in Liquid Phase
Nylon	0.0052	7.52×10^{-12}	1.44×10^{-10}
Polystyrene	0.0042	1.05×10^{-9}	1.44×10^{-9}
LDPE	0.0019	1.31×10^{-9}	1.80×10^{-9}
PDMS	0.0170	3.24×10^{-7}	1.16×10^{-7}
PDMS	0.0273	3.23×10^{-7}	1.68×10^{-7}
PDMS	0.0526	3.07×10^{-7}	2.04×10^{-7}
PDMS	0.1114	2.81×10^{-7}	3.52×10^{-7}

[a] Units: $P/cm^3(STP)cmcm^{-2}s^{-1}cmHg^{-1}$.

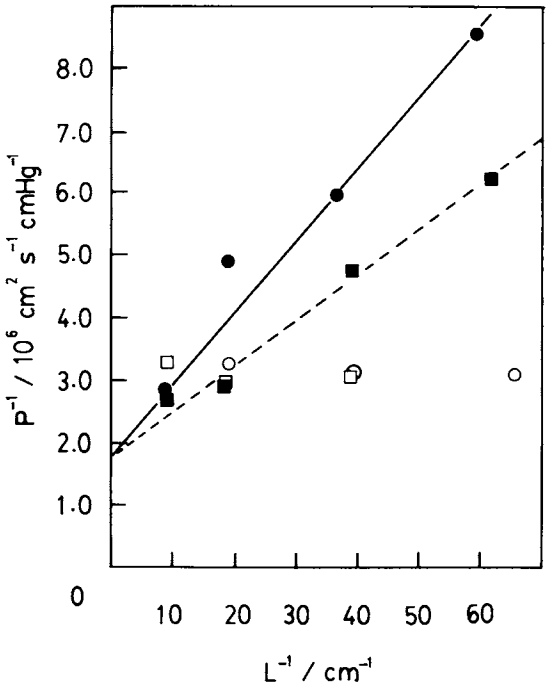

Figure 6 Plots of P^{-1} vs. L^{-1} for nontreated PDMS (●) and plasma-treated PDMS (■) membranes in liquid phase and for nontreated PDMS (○) and plasma-treated PDMS (□) membranes in gas phase. The condition of plasma treatment is 10 W for 1 min.

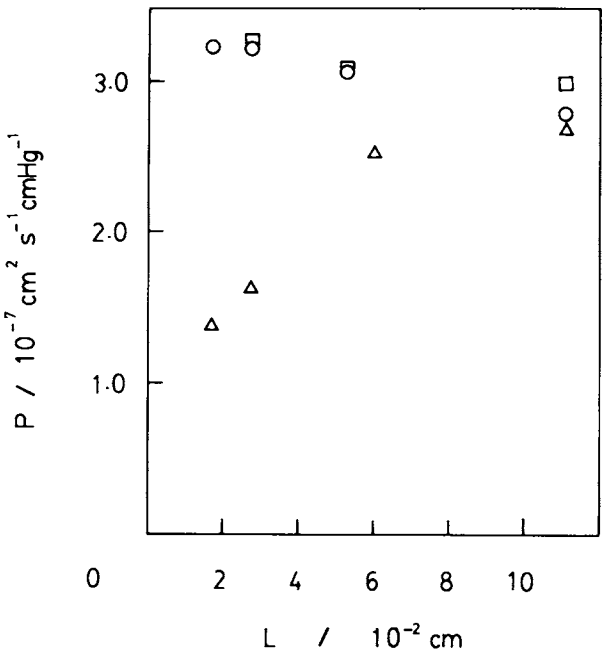

Figure 7 Dependence of permeability coefficients of CO_2 on membrane thickness for plasma-treated [(□) 10 W for 1 min; (△) 50 W for 1 min] and nontreated PDMS membranes (○) in gas phase.

membrane surfaces and makes the surfaces crosslinked.[13] We intended to examine whether the permeability coefficients in plasma-treated PDMS membranes were different from those in nontreated PDMS membranes where the resistance on the surfaces of plasma-treated PDMS due to crosslinking was negligibly small.

Two types of plasma-treated PDMS membranes (10 W for 1 min and 50 W for 1 min) were prepared for this purpose. Figure 7 shows the dependence of permeability coefficients on each membrane thickness for the plasma-treated and the nontreated PDMS membranes in the gas phase.

The permeability coefficients in the plasma-treated membranes at 50 W for 1 min are found to decrease with decreasing the membrane thickness, while those in the membranes treated at 10 W for 1 min show independence of membrane thickness and agree with the permeability coefficients in nontreated PDMS membranes in the gas phase. The latter membranes (10 W for 1 min) were, therefore, used in the following experiments.

Figure 6 also shows plots of P^{-1} vs. $1/L$ for the plasma-treated PDMS membranes. It is obvious that the slope for the plasma-treated membranes is smaller than that for the nontreated membranes, but the intercepts for plasma-treated and nontreated membranes agree within the experimental error. DS and R_w are also calculated for the plasma-treated PDMS membranes and are summarized in Table II. DS's are observed not to be different between the plasma-treated and nontreated membranes from the

Table II Dissolved Carbon Dioxide Permeabilities in PDMS Membranes and Boundary Layer Thickness at 25°C[a]

Membranes	DS	P in Gas Phase	R_w	$L_w/\mu m$
Nontreated PDMS	5.52×10^{-7}	3.14×10^{-7}	1.16×10^5	220
Plasma-treated PDMS	5.52×10^{-7}	3.14×10^{-7}	0.727×10^5	138

[a] Units: DS/cm^3(STP)$cmcm^{-2}s^{-1}cmHg^{-1}$, P/cm^3(STP)$cmcm^{-2}s^{-1}cmHg^{-1}$, R_w/cm^{-3}(STP)cm^2s cmHg.

table. The boundary layer resistance for the plasma-treated membranes is, however, found to be smaller than that for the nontreated membranes. The boundary layer thickness is estimated to be 220 μm for the nontreated membrane and 138 μm for the plasma-treated membrane on the assumption that the permeability coefficient of dissolved CO_2 in the boundary layer is the same with that in bulk water, 1.9×10^{-7} $cm^3(STP)cm/cm^2$ s cm Hg, which is calculated from diffusion and solubility coefficients of CO_2 in bulk water (i.e., 1.9×10^{-5} cm^2/s[18] 0.0100 $cm^3(STP)/cm^3$ cm Hg[14]) at 25°C. The boundary layer thickness for the membranes having hydrophilic surfaces (plasma-treated membranes) is, therefore, observed to be less than that for the membranes having hydrophobic surfaces (nontreated membranes). The mild-plasma treatment is, therefore, found to be effective in increasing the apparent permeability coefficient in the liquid phase.

Yang et al.[1] reported that dissolved oxygen permeability coefficients for poly(vinyl alcohol) and some other membranes at 34°C. DS and R_w for PVA-1 are calculated to be 8.70×10^{-7} $cm^3(STP)cm/cm^2$ s cm Hg and 2.24×10^5 $cm^{-3}(STP)cm^2$ s cm Hg that corresponds to 147 μm of the boundary layer thickness. Their cell was stirred at 450 rpm which was a similar speed to our case (430 rpm). It may be difficult to compare with the boundary layer thickness for the CO_2 permeability coefficient in plasma-treated PDMS (138 μm) and that for the O_2 permeability coefficient in PVA (147 μm), though it is found that there is no great difference in the boundary layer thickness in the case where permeant species are different.

It is concluded that the boundary layer thickness for the hydrophilic surfaces is thinner than that for the hydrophobic surfaces. Very mild-plasma treatment (10 W for 1 min in our case) which makes the hydrophilic surfaces without change of bulk polymer materials will be effective in decreasing the boundary layer thickness and to increase the apparent permeability in the liquid phase.

REFERENCES

1. W. Yang, V. F. Smolen, and N. A. Peppas, *J. Membrane Sci.*, **9**, 53 (1981).
2. C. O. Ng and B. J. Tighe, *Br. Polym. J.*, **8**, 118 (1976).
3. S. Hosaka et al., *Kobunshi Ronbunshu*, **36**, 265 (1979).
4. M. F. Refojo and F. L. Leong, *J. Membrane Sci.*, **4**, 415 (1979).
5. M. J. Juarequi and I. Fatt, *Am. J. Optom.*, **48**, 210 (1971).
6. S. T. Hwang, T. E. S. Tang, and K. Kammermeyer, *J. Macromol. Sci. Phys.*, **B5**(1), 1 (1971).
7. B. Tang, T. Masuda, and T. Higashimura, *J. Polym. Sci. Polym. Phys.*, **27**, 1261 (1989).
8. A. Higuchi, M. Abe, J. Komiyama, and T. Iijima, *J. Membrane Sci.*, **21**, 113 (1984).
9. A. Higuchi, H. Fushimi, and T. Iijima, *J. Membrane Sci.*, **25**, 171 (1985).
10. W. Z. Zhang, M. Satoh, and J. Komiyama, *J. Membrane Sci.*, **31**, 147 (1987).
11. W. Z. Zhang, A. Nodera, M. Satoh, and J. Komiyama, *J. Membrane Sci.*, **35**, 311 (1988).
12. J. Izydorczyk, J. Podkòwka, and J. Salwiński, *J. Membrane Sci.*, **2**, 235 (1977).
13. H. Yasada, H. C. Marsh, S. Brandt, and C. N. Reilley, *J. Polym. Sci. Polym. Chem.*, **15**, 991 (1977).
14. *Kagaku Binran, Kisohen (Handbook of Chemistry, Basic Ed.)*, Maruzen, Japan, 1980, pp. 769–770.
15. Technical Report for CE-235, TOA Electronics Ltd., Japan.
16. G. T. Paulson, A. B. Clinch, and F. P. McCandless, *J. Membrane Sci.*, **14**, 129 (1983).
17. S. Zhou and S. A. Stern, *J. Polym. Sci. Polym. Phys.*, **27**, 205 (1989).
18. International Critical Tables, National Research Council, McGraw-Hill, New York, Vol. 5, 1933.

Received November 13, 1989
Accepted March 21, 1990